

Equation of state in hybrid stars and the stability window of quark matter

Xin-Jian Wen

Department of Physics and Institute of Theoretical Physics, Shanxi University, Taiyuan 030006, China

Abstract

Properties of hybrid stars with a mixed phase composed of asymmetric nuclear matter and strange quark matter are studied. The quark phase is investigated by the quark quasiparticle model with a self-consistent thermodynamic and statistical treatment. We present the stability windows of the strange quark matter with respect to the interaction coupling constant versus the bag constant. We find that the appearance of the quark-hadron mixed phases is associated with the meta-stable or unstable regions of the pure quark matter parameters. The mass-radius relation of the hybrid star is dominated by the equation of state of quark matter rather than nuclear matter. Due to the appearance of mixed phase, the mass of hybrid star is reduced to $1.64 M_{\odot}$ with radius 10.6 km by comparison with neutron star.

Keywords: Thermodynamic and statistical physics of quasiparticle model; Equation of state of strange quark matter; Phase diagram of hybrid stars

1. INTRODUCTION

The appearance of quark matter or hadron-quark mixed phase in the massive neutron stars is a hot topic in the study of compact objects. The baryon densities of the stars cover a larger range from very low densities in the outer part to the order of about ten times the saturation density in the inner core. To study the structure of compact stars, the key point is to find a reliable form of the equation of state (EOS) that determines the characteristic of the constituent matter [1]. Unfortunately, however, there is no single theory to cover the large density range with respect to quark degrees of freedom. In literature, the low-density phase can be described by quantum hydrodynamics (QHD). At high densities, a new form of matter, called strange quark matter (SQM), might exist and be more stable than nuclear matter (^{56}Fe) [2, 3, 4, 5, 6]. For more theoretical and experimental results, see [7, 8, 9, 10]. A family of compact stars consisting completely of the deconfined mixture of u -, d -, s - quarks has been called “strange stars” [11, 12, 13]. If the hypothesis of stable strange quark matter is correct [3], the possibility of phase transition exists in principle [14]. The compact star with a “quark matter core”, either as a hadron-quark mixed phase or as a pure quark phase, are called “hybrid stars” (HyS) [15, 16]. Recently, it was argued that the interior core of a low-mass compact star could be dominated by the Color-Flavor-Locked

Email address: wenxj@sxu.edu.cn (Xin-Jian Wen)

(CFL) quark matter [17, 18]. In contrast, it was remarked that the CFL phase would make the HyS unstable [19] and the possible configuration of compact stars, such as the strange hadrons, hyperonic matter [20] and quark matter core, can soften the equation of states of neutron stars [20, 21, 22]. However, Alford et al pointed out the “masquerade effect” [23] that the hybrid star has a mass-radius relation similar to that of the pure neutron star. Also, the isolated neutron star RX J1856-375 with a large radius and/or mass [24] is a possible candidate of HyS, which implies a constraint on testing a rather stiff equation of state at high density [25]. Regardless of whether the quark matter is ruled out, it seemed that the soft equation of state were ruled out in the center of compact stars [26].

To get a reliable equation of state in the microscopic calculation of interacting dense hadronic matter, Wiringa et.al added the three-body potential to the nucleon Hamiltonian and gave the light nuclei binding energy and nuclear matter saturation properties [27]. The Brueckner theory with three-body forces has been used recently to study the mixed phase of hadrons and quarks in compact stars [28]. In literature, there is another successful method called relativistic mean-field (RMF) theory. It is a powerful tool in describing various aspects of nuclear physics, such as the properties of nuclear matter, finite nuclei, and neutron stars, as well as the dynamics of heavy-ion collisions [29, 30]. Recently, the model has been extended to include the density-dependent meson-nucleon coupling constant in finite nuclei [31] and nuclear matter [25, 32].

In the theoretical description of the deconfined quark matter, we can resort to the phenomenological models constrained by experimental information. There are many successful works considering the medium-effect of quark masses. One of them obtains the confinement by the density dependence of quark masses [33]. Another one is the quark quasiparticle model, where the vacuum energy density is not constant but density-dependent. For the medium dependence of the quasiparticle masses, it was derived at the zero-momentum limit of the dispersion relations from an effective quark propagator by resumming one-loop self-energy diagrams in the hard-dense-loop approximation (HDL) [34]. We have recently extended the model to include the important finite-size effect [35] and magnetized strange quark matter (MSQM) [36].

In this paper, we study the effect of the interaction coupling constants on the equation of mixed phase of nuclear and quark matter and the properties of hybrid stars. For the nuclear EOS, we adopt the relativistic nuclear field theory solved at the mean-field level, and especially the Baym-Pethick-Sutherland (BPS) model for densities below $5 \times 10^{14} \text{g cm}^{-3}$ [37, 38]. In describing quark matter, we employ the quark quasiparticle model instead of the conventional bag model [22]. The density-dependent bag function is obtained self-consistently rather than artificially.

This paper is organized as follow. In Section 2, we briefly give a short introduction to the relativistic nonlinear mean-field model describing the nuclear matter. In Section 3, we introduce the treatment of SQM in the framework of the quark quasiparticle model and present the stability window of quark matter. In Section 4, we display the phase diagram of the mixed phase and discuss the chemical potential behavior. With the equations of state, we investigate the influence of coupling constant and bag constant on the mass-radius relation. The last section is a short summary.

2. The nuclear EOS in the relativistic mean-field model

The relativistic nuclear field theory is solved at the mean-field level. The in-medium interaction of nucleons can be realized through the exchanges of the σ , ω , and ρ mesons. The bulk matter is assumed to be electrically neutralized and in the lowest energy state, i.e. in general

β -equilibrium. The influence of the temperature can be neglected [39]. The Lagrange density for this model is written as [40, 41]

$$\begin{aligned}\mathcal{L}_{RMF} = & \frac{1}{2}(\partial_\mu\sigma\partial^\mu\sigma + m_\rho^2\rho_\mu\rho^\mu) - U(\sigma) + V(\omega) - \frac{1}{4}[\Omega_{\mu\nu}\Omega^{\mu\nu} + R_{\mu\nu}^a R^{a\mu\nu} + F_{\mu\nu}F^{\mu\nu}] \\ & + \bar{\psi}\left(i\gamma^\mu\partial_\mu - m_N + g_{\sigma N}\sigma - g_{\omega N}\gamma^\mu\omega_\mu - \frac{1}{2}g_{\rho N}\gamma^\mu\rho_\mu^a \cdot \tau^a - e\gamma^\mu Q_e A_\mu\right)\psi \\ & + \bar{\psi}_e(i\gamma^\mu\partial_\mu - m_e)\psi_e.\end{aligned}\quad (1)$$

where the nucleon field ψ has a form of column vector for protons and neutrons, and the field tensors are given by

$$\Omega_{\mu\nu} = \partial_\nu\omega_\mu - \partial_\mu\omega_\nu, \quad (2)$$

$$R_{\mu\nu}^a = \partial_\mu\rho_\nu^a - \partial_\nu\rho_\mu^a, \quad (3)$$

$$F_{\mu\nu} = \partial_\nu A_\mu - \partial_\mu A_\nu. \quad (4)$$

The non-linear potential functions are contained for the meson σ [42] and ω as

$$U(\sigma) = \frac{1}{2}m_\sigma^2\sigma^2 + \frac{1}{3}g_3\sigma^3 + \frac{1}{4}g_4\sigma^4, \quad (5)$$

$$V(\omega) = \frac{1}{2}m_\omega^2\omega_\mu\omega^\mu + \frac{1}{4}c_4(\omega_\mu\omega^\mu)^2. \quad (6)$$

The parameters m_N , m_σ , m_ρ , m_ω are the masses of nucleon, scalar meson σ , isovector-vector meson ρ , and isoscalar-vector meson ω respectively. In principle, they can be fixed algebraically by the properties of bulk nuclear matter, such as, the binding per nucleon, the saturation baryon density, the effective mass of the nucleon at saturation, and the compression modulus. The isovector ρ field vanishes for symmetry nuclear matter.

The scalar density and conserved baryon number density are expressed with the use of Fermi integrals

$$\rho_s = \frac{4}{(2\pi)^3} \int_0^{p_f} \frac{M^*}{\sqrt{p^2 + M^{*2}}} dp^3, \quad (7)$$

$$\rho_N = \rho_p + \rho_n = \frac{v_p^3}{3\pi^2} + \frac{v_n^3}{3\pi^2}, \quad (8)$$

where the effective nucleon mass is defined by $M^* \equiv M - g_{\sigma N}\sigma_0$, with v_p and v_n being the Fermi momenta of protons and neutrons respectively.

The energy density and pressure of nuclear matter can be obtained from the energy-momentum tensor. Including the contribution of nucleons and mesons, the total energy density ϵ^{HP} and the pressure P^{HP} are [15, 43]

$$\begin{aligned}\epsilon^{\text{HP}} = & \frac{2}{(2\pi)^3} \left[\int_0^{v_p} \sqrt{p^2 + M^{*2}} dp^3 + \int_0^{v_n} \sqrt{p^2 + M^{*2}} dp^3 \right] \\ & + \frac{1}{2}m_\sigma^2\sigma^2 + \frac{1}{3}g_3\sigma^3 + \frac{1}{4}g_4\sigma^4 + \frac{1}{2}m_\omega^2\omega_0^2 + \frac{3}{4}c_4\omega_0^4 + \frac{1}{2}m_\rho^2\rho_0^2, \quad (9) \\ P^{\text{HP}} = & \frac{1}{3} \frac{2}{(2\pi)^3} \left[\int_0^{v_p} \frac{p^2}{\sqrt{p^2 + M^{*2}}} dp^3 + \int_0^{v_n} \frac{p^2}{\sqrt{p^2 + M^{*2}}} dp^3 \right]\end{aligned}$$

$$-\frac{1}{2}m_\sigma^2\sigma^2 - \frac{1}{3}g_3\sigma^3 - \frac{1}{4}g_4\sigma^4 + \frac{1}{2}m_\omega^2\omega_0^2 + \frac{1}{4}c_4\omega_0^4 + \frac{1}{2}m_\rho^2\rho_0^2. \quad (10)$$

If the electron contribution is included, $P_e = \mu_e^4/(12\pi^2)$. For symmetric nuclear matter, the number density of protons and neutrons are equal, and correspondingly the Fermi momenta are also equal, i.e., $\nu_p = \nu_n$. In this case, the isovector meson has no contribution.

From the equation of motion for nucleons, the Fermi energy of nucleons, or equivalently, the chemical potential μ_N can be expressed as

$$\mu_N = g_{\omega N}\omega_0 + \frac{1}{2}g_{\rho N}\rho_0\tau_{3N} + \sqrt{\nu^2 + M^{*2}}. \quad (11)$$

In this paper, we choose four typical sets of parameters (TM1, NL3, BKA20, and TW-99) [32, 44]. They stand for different stiffness equations of state. The masses for σ , ω , and ρ mesons are $m_\sigma = 509\text{MeV}$, $m_\omega = 782\text{MeV}$, and $m_\rho = 770\text{MeV}$ with nucleon mass $M = 939\text{MeV}$. For getting the EOS in the low-density, i.e., the crust equation of state of compact stars, we can resort to the BPS model [37] in calculations.

3. Quark quasiparticle model for quark matter EOS

At high density, nuclear matter is expected to undergo a phase transition to a deconfined phase. If the quark chemical potential exceeds the strange quark mass, the system can lower its Fermi energy by converting the down quark into strange quarks. Recently, we have developed the quark quasiparticle model in studying strangelets [35] and MSQM [36]. In the quasiparticle model, the effective quark mass following from the hard-dense-loop (HDL) approximation of quark self-energy at zero temperature is expressed as [34, 45],

$$m_i^* = \frac{m_i}{2} + \sqrt{\frac{m_i^2}{4} + \frac{g^2\mu_i^2}{6\pi^2}}, \quad (12)$$

where m_i is the corresponding current mass of quarks, $g = \sqrt{4\pi\alpha_s}$ denotes the strong interaction coupling constant. The effective quark mass m_i^* increases with g , m_i and the quark chemical potential μ_i . In this paper, we treat g as a free parameter in the range of $(0, 5)$. For light quarks (u and d quarks), we take the current mass to be zero, and Eq. (12) is reduced to the simple form

$$m_i^* = \frac{g\mu_i}{\sqrt{6}\pi} \equiv \alpha\mu_i, \quad (i = u, d) \quad (13)$$

The quasiparticle contribution to the thermodynamic potential density is given as [35].

$$\Omega_i = -\frac{d_i T}{2\pi^2} \int_0^\infty \left\{ \ln \left[1 + e^{-(\epsilon_{i,p} - \mu_i)/T} \right] + \ln \left[1 + e^{-(\epsilon_{i,p} + \mu_i)/T} \right] \right\} p^2 dp, \quad (14)$$

where $\epsilon_{i,p} = \sqrt{p^2 + m_i^{*2}}$ and T is the temperature. At zero temperature, the integration can be calculated out to give

$$\Omega_i = -\frac{d_i}{48\pi^2} \left[|\mu_i| \sqrt{\mu_i^2 - m_i^{*2}} (2\mu_i^2 - 5m_i^{*2}) + 3m_i^{*4} \ln \frac{|\mu_i| + \sqrt{\mu_i^2 - m_i^{*2}}}{m_i^*} \right], \quad (15)$$

where m_i and μ_i are, respectively, the particle masses and chemical potentials. d_i is the degeneracy factor with $d_i = 2(\text{spin}) \times 3(\text{color}) = 6$ for quarks and $d_i = 2$ for electrons. When the variable set $(T, V, \{\mu_i\})$ is chosen as the independent state variables, the thermodynamic potential is the characteristic function. In the quasiparticle model, the total thermodynamic potential density can be written as

$$\Omega = \sum_i [\Omega_i(\mu_i, m_i^*) + B_i(\mu_i)] + B_0, \quad (16)$$

Where $B_i(\mu_i)$ is the medium-dependent quantity determined by thermodynamic consistency. A little later, we will see that $B_i(\mu_i)$ is given by an indefinite integration. When it is expressed by a definite integration, an integration constant is needed. Therefore, B_0 is from the sum of relevant integration constants, and we treat it as a free input parameter. In the quasiparticle model, the particle number density should be of the same form as that of a Fermi gas with the normal particle mass replaced by the effective quasiparticle mass, i.e.,

$$n_i = -\frac{\partial \Omega_i}{\partial \mu_i} = \frac{d_i}{6\pi^2} (\mu_i^2 - m_i^{*2})^{3/2}. \quad (17)$$

On the other hand, we know from the fundamental thermodynamics that

$$n_i = -\left. \frac{d\Omega}{d\mu_i} \right|_{\mu_{k \neq i}} = -\frac{\partial \Omega_i}{\partial \mu_i} - \frac{\partial \Omega_i}{\partial m_i^*} \frac{\partial m_i^*}{\partial \mu_i} - \frac{dB_i}{d\mu_i}. \quad (18)$$

Equating the last equality in Eq. (18) with the first equality in Eq. (17), we immediately have

$$\frac{dB_i}{d\mu_i} = -\frac{\partial \Omega_i}{\partial m_i^*} \frac{\partial m_i^*}{\partial \mu_i} \quad \text{i.e.} \quad B_i = -\int_{m_i^*}^{\mu_i} \frac{\partial \Omega_i}{\partial m_i^*} \frac{\partial m_i^*}{\partial \mu_i} d\mu_i, \quad (19)$$

where the derivative of the thermodynamic potential density with respect to the quark effective mass can be analytically expressed by

$$\frac{\partial \Omega_i}{\partial m_i^*} = \frac{d_i m_i^*}{4\pi^2} \left[\mu_i \sqrt{\mu_i^2 - m_i^{*2}} - m_i^{*2} \ln \frac{\mu_i + \sqrt{\mu_i^2 - m_i^{*2}}}{m_i^*} \right]. \quad (20)$$

Accordingly, the pressure P^{QP} , energy density ϵ^{QP} , and baryon density ρ^{QP} for SQM at zero temperature are written as,

$$P^{\text{QP}} = -\sum_i [\Omega_i(\mu_i, m_i^*) + B_i(\mu_i)] - B_0, \quad (21)$$

$$\epsilon^{\text{QP}} = \sum_i [\Omega_i(\mu_i, m_i^*) + B_i(\mu_i)] + \sum_i \mu_i n_i + B_0, \quad (22)$$

$$\rho^{\text{QP}} = \frac{1}{3} \sum_i n_i. \quad (23)$$

Because the current mass of light quarks is nearly zero, one can have an analytical expression for light quarks by combining Eqs. (13) and (19) [35, 34], giving

$$\begin{aligned} B_i^*(\mu_i) &= -\int_0^{\mu_i} \left. \frac{\partial \Omega}{\partial m_i^*} \right|_{T=0, \mu_i} \frac{dm_i^*}{d\mu_i} d\mu_i \\ &= -\frac{d_i}{16\pi^2} \left[\alpha^2 \beta - \alpha^4 \ln \left(\frac{\beta + 1}{\alpha} \right) \right] \mu_i^4, \quad (i = u, d), \end{aligned} \quad (24)$$

where $\alpha = g/(\sqrt{6}\pi)$ and $\beta = \sqrt{1 - \alpha(g)^2}$ are g -dependent functions.

For massive quarks, $B^*(\mu)$ has been observed as the result [34],

$$B_s^*(\mu_s) = -\frac{d_s}{16\pi^2} \left[\frac{\sqrt{(m_s^* - m_s)(\beta^2 m_s^* - m_s)}}{24\alpha^2 \beta^4} \right] \times \sum_{n=0}^3 a_n m_s^{3-n} m_s^{*n} - m_s^{*4} \ln \left(\frac{k_F + \mu}{m_s^*} \right) + \frac{5\alpha^4 - 12\alpha^2 + 8}{16\beta^5} m_s^4 \times \ln \left(\frac{\beta \sqrt{m_s^* - m_s} + \sqrt{\beta^2 m_s^* - m_s}}{\alpha^2 m_s} \right), \quad (25)$$

where the coefficient a_n can be related to the coupling constant through four polynomial function as in [34], which is very different from the gaussian parametrization of the density-dependent bag constant [46].

With the above quark mass formulas and thermodynamic treatment, one can get the properties of bulk quark matter. According to the Witten-Bodmer hypothesis, it is required that the energy per baryon of two-flavor quark matter is bigger than 930 MeV in order not to contradict with standard nuclear physics, but that of symmetric three-flavor quark matter is less than 930 MeV. For the co-existence of nuclear matter and quark matter in the process of phase transition, the allowed values of model parameters should be chosen in the metastable or unstable regions. In Fig. 1, we present the stability windows of SQM in the $B_0^{1/4}$ - g plane. The area below the dotted line is forbidden because the energy per baryon ϵ^{QP}/ρ^{QP} of 2-flavor quark matter is less than 930 MeV. The ϵ^{QP}/ρ^{QP} of 3-flavor quark matter is smaller than 930 MeV below the solid line and is smaller than 939 MeV in the narrow area below the dashed line. In the top area the strange quark matter is unstable.

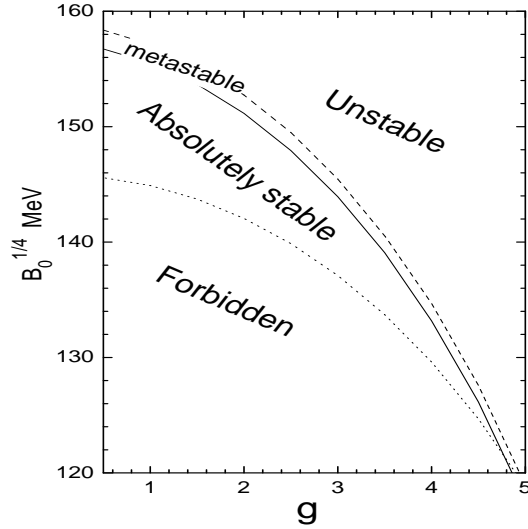


Figure 1: Stability windows in the parameter space ($B_0^{1/4}$, g). Below the dotted line is the forbidden area where two-flavor quark matter is absolutely stable. Above the solid or dashed line, SQM is meta-stable or unstable, and SQM is absolutely stable between the the dotted and solid curves.

4. Hadron-quark mixed phase and hybrid stars

4.1. Transition from nuclear matter to quark matter

We suppose that the compact star composed of quark matter core and nuclear matter surface. The nuclear matter includes protons, neutrons and electrons. The quark matter consists of a mixture of quarks (u , d , and s) and electrons. In the interface of the two phases, there may be a mixed phase of nuclear and quark matter, which is important in understanding the properties of hybrid stars. To describe the structure of the mixed phase, we define the fraction χ occupied by quark matter by $\chi \equiv V^{\text{QP}}/(V^{\text{QP}} + V^{\text{HP}})$. Then we have the total baryon number density ρ , energy density ϵ , and electrical charge Q as,

$$\rho_B = (1 - \chi)\rho^{\text{HP}} + \chi\rho^{\text{QP}}, \quad (26)$$

$$\epsilon = (1 - \chi)\epsilon^{\text{HP}} + \chi\epsilon^{\text{QP}}, \quad (27)$$

$$Q = (1 - \chi)Q^{\text{HP}} + \chi Q^{\text{QP}}, \quad (28)$$

where $Q = 0$ according to the bulk charge neutrality requirement. The critical density ρ_c^{HP} for pure nuclear matter is determined by $\chi = 0$. With increasing density, the deconfinement phase transition takes place. Consequently, quark matter appears in the mixed phase. When χ increases up to 1, the quark phase dominates the system completely at the critical density ρ_c^{QP} .

From the quark constituent of nucleons, we have the chemical potential relations through the linear combinations,

$$\mu_p = 2\mu_u + \mu_d, \quad \mu_n = \mu_u + 2\mu_d. \quad (29)$$

Incorporated with the β -equilibrium condition $\mu_d = \mu_s = \mu_u + \mu_e$, there are only two independent chemical potentials, e.g. μ_u and μ_e . The Gibbs condition for the phase equilibrium between nuclear matter and quark matter is that the system should be in thermal, chemical, and mechanical equilibrium. Therefore, in addition to the common zero temperature, we also have the two conditions

$$\mu^{\text{HP}} = \mu^{\text{QP}}, \quad (30)$$

$$P^{\text{HP}}(\mu_p, \mu_n, \mu_e) = P^{\text{QP}}(\mu_u, \mu_d, \mu_s, \mu_e), \quad (31)$$

where P^{HP} and P^{QP} denotes the pressure in the nuclear phase and in the quark phase, respectively. They are given by Eqs. (10) and (21) separately. The electron is uniformly distributed in the system and the pressure is common for both phases. Eq. (30) means that the baryon chemical potential in both phases are the same. It can be shown that Eq. (30) is equivalent to Eq. (29) [28]. For a given total baryon number density, one can obtain the two independent chemical potentials and χ by solving the equations (26), (28) and (31).

In Fig. 2, the system energy per baryon is displayed as a function of the density for $g = 3$, $B_0^{1/4} = 150$ MeV, and TM1 parameter set. The mixed phase (shaded area) exists in the range of about 1 ~ 3 times the nuclear saturation density. In this density range, the energy per baryon of mixed phase (solid line) is lower than that of both the pure nuclear (dashed line) and the pure quark phase (dotted line). So the appearance of the mixed phase in neutron star matter is energetically favored for a proper parameter in meta-stable or unstable regions. This observation is consistent with that in Ref. [28]. If one chooses the absolutely stable parameter-sets ($g, B_0^{1/4}$), no mixed phase will exist and the hybrid star is unstable and will collapse to a strange star. In the middle density range, the mixed phase starts at the nuclear critical density ρ_c^{HP} where $\chi = 0$ and

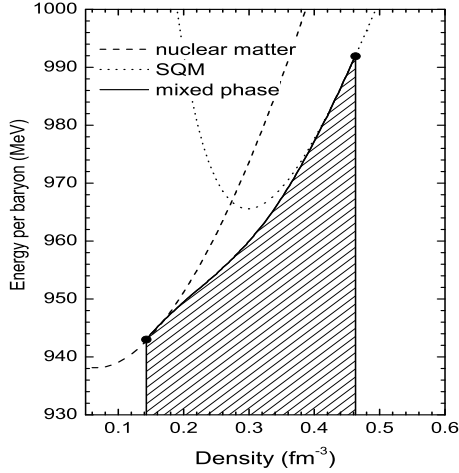


Figure 2: The energy per baryon as a function of density. In the density range of shaded area, the energy per baryon (solid line) is lower than that of either quark matter (dotted line) or nuclear matter (dashed line). $g = 3$, $B_0^{1/4} = 150$ MeV, and TM1 set are adopted.

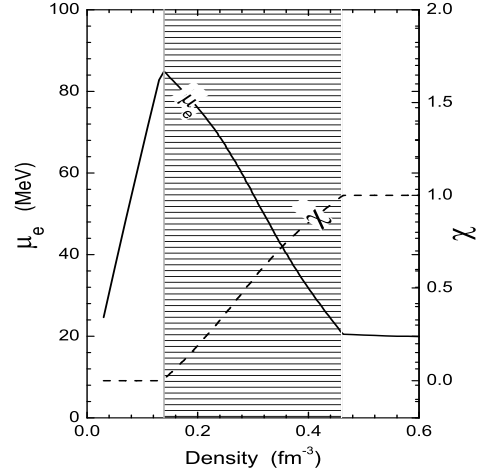


Figure 3: The electron chemical potential μ_e (left axis) and the fraction of SQM χ (right axis). Parameters are the same as for Fig. 2.

ends at the quark critical density ρ_c^{QP} where $\chi = 1$. The critical points are marked with full dots in Fig. 2. By comparing the different equation of state for nuclear matter, we find that the solid lines between the ρ_c^{HP} and ρ_c^{QP} is shorter for harder EOS of nuclear matter. It is also observed that the quark critical density ρ_c^{QP} varies only slightly with the RMF parameters.

To provide a better understanding of the Glendenning hypothesis of global charge neutrality, we give the electron chemical potential and the quark fraction versus the total density in Fig. 3. In the shaded area of mixed phase, the increasing contribution of quark phase is a complementarity to the decrease of electrons. The electron chemical potential μ_e (dashed line) decreases rapidly from the maximum value 85 MeV to 20 MeV. And finally it becomes very small in the pure quark phase where the quark fraction χ is unity, where the three-flavor quark matter occupies the whole space.

4.2. The structure of hybrid stars

With the above equation of state, we now study the structure of compact stars. As usually done, we assume that the hybrid star is a spherically symmetric distribution of mass in hydrostatic equilibrium. The equilibrium configurations are obtained by solving the Tolman-Oppenheimer-Volkoff (TOV) equation for the pressure $P(r)$, the energy density $\epsilon(r)$ and the enclosed mass $m(r)$:

$$\frac{dP(r)}{dr} = -\frac{Gm(r)\epsilon(r)}{r^2} \frac{[1 + P(r)/\epsilon(r)][1 + 4\pi r^3 P(r)/m(r)]}{1 - 2Gm(r)/r} \quad (32)$$

where $G = 6.707 \times 10^{-45} \text{MeV}^{-2}$ is the gravitational constant, r is the distance from the center of the star. The subsidiary condition is

$$\frac{dm(r)}{dr} = 4\pi r^2 \epsilon(r). \quad (33)$$

Giving the stellar radius R , which is defined by zero pressure at the stellar surface, the gravitational mass is given by

$$M(R) \equiv 4\pi \int_0^R r^2 \epsilon(r) dr. \quad (34)$$

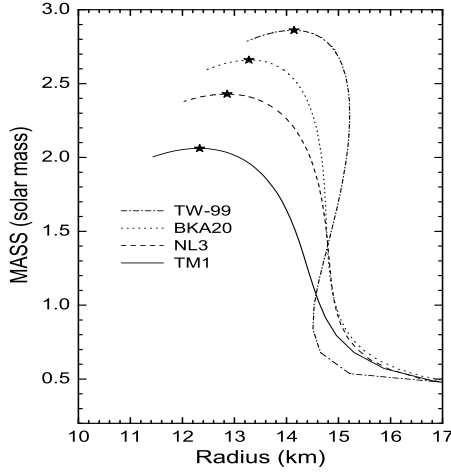


Figure 4: The mass-radius relation of neutron stars. The maximum mass is marked with an asterisk on each curve.

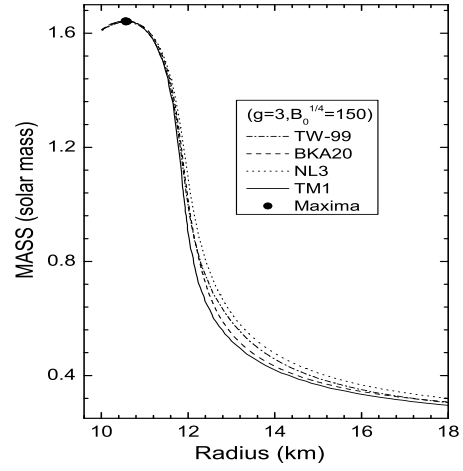


Figure 5: The mass-radius relation of hybrid stars with different parameter sets of the nuclear matter. The maximum mass, marked with a full dot on each curve, do not change significantly with the nuclear parameters.

Before investigating the properties of the hybrid star, let's give the mass-radius relations for compact stars composed of pure nuclear matter. The TOV equation is solved with the nuclear matter EOS introduced in Sec. 2. We take the four parameter sets in the calculation: TM1, NL3, BKA20, TW-99. The maximum masses of neutron stars are located in 2 ~ 3 times the solar mass M_\odot with the corresponding radii in the range (12.3 ~ 14.1 km) in Fig. 4. For harder EOS of the parameter set TW-99, the maximum star mass approaches the value 2.86 M_\odot , which is bigger than the mass 2.06 M_\odot with the parameter set TM1. Different with the self-bound stars, the equation of state of nuclear matter at lower density is calculated in the BPS model.

To investigate the influence of model parameter on the mass-radius relation of hybrid stars, we should consider different EOS of the nuclear matter and strange quark matter. Firstly, the parameter set ($g = 3$, $B_0^{1/4} = 150 \text{ MeV}$) is employed on the quark side, while different parameter sets on the nuclear side are adopted in the calculation. The corresponding mass-radius relations are plotted in Fig. 5 where the maximum star mass are marked with full dots. Even though the nuclear parameter is adopted for different sets, the maximum mass is very close to the same value 1.64 M_\odot . Doing calculations with other choices of the parameter B_0 and g , we find the

result that the maximum mass does not be significantly influenced by the parameter uncertainty of the nuclear equation of state.

Now we fixed the TM1 parameter set for the nuclear EOS while changing the values of g and B_0 on the quark side. In this case the maximum mass of hybrid stars is calculated in Fig. 6. The distinction between Fig. 5 and 6 can be understood from the comparison of EOS. In the upper panel of Fig. 7, we can know that the narrow range on the energy density axis is affected by nuclear parameter sets, while a larger range is greatly dominated by quark matter parameter sets. For a bigger value of the maximum of hybrid stars, the corresponding density range of the mixed phase is wider. In the parameter range, the maximum mass is in the range $(1.5 \sim 2.04)M_\odot$ and radius in the range $(9.64 \sim 12.4)$ km, which comprises the pulsar PSR J1614-2230 with $1.97 \pm 0.04M_\odot$ [47]. For a completely relation between the maximum mass of hybrid stars and the parameter set of SQM, we show the contour plots of the maximum mass in the panel with $B_0^{1/4}$ and g on the horizontal and vertical axis in Fig. 8. According to the stability window shown in Fig. .1, the maximum mass of hybrid stars has been marked on each line in the allowed area.

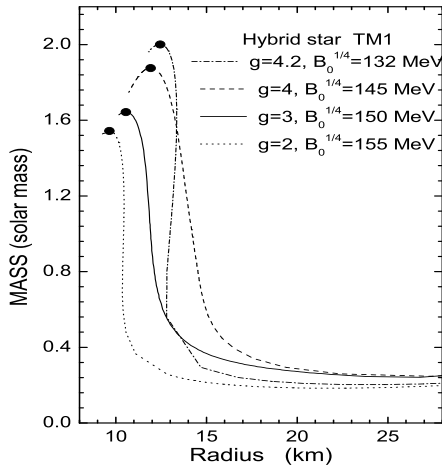


Figure 6: The mass-radius relation of hybrid stars with various parametrization of quark matter. The maximum masses are marked with full dots.

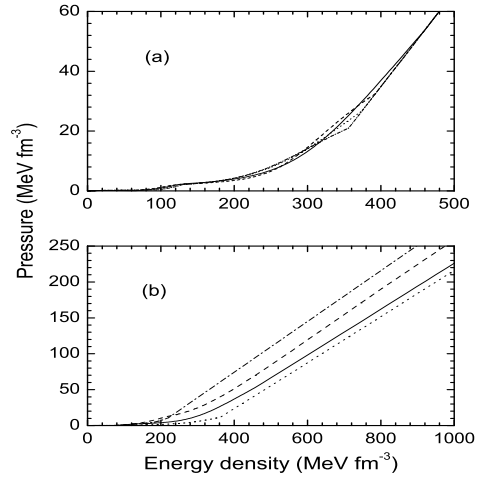


Figure 7: The pressure versus the energy density for the equations of state of hybrid stars. Figure (a) and (b) are, respectively, for Fig. 5 and 6.

5. Summary

We have studied the hybrid stars with mixed phase of nuclear matter and SQM. In the outer layer, the nuclear matter is described by the relativistic mean-field theory and crust EOS by the BPS model. In the inner core, the quark matter is investigated by the quasiparticle model. According to the Witten-Bodmer hypothesis, we present the stability window of quark matter in the coupling constant g versus bag constant $B_0^{1/4}$ panel. The mixed phase exists in the range 1 \sim 3 times the nuclear saturation density, which is energetically favorable by comparison with pure nuclear matter or SQM. We point that the mixed phase of hybrid stars is located in the

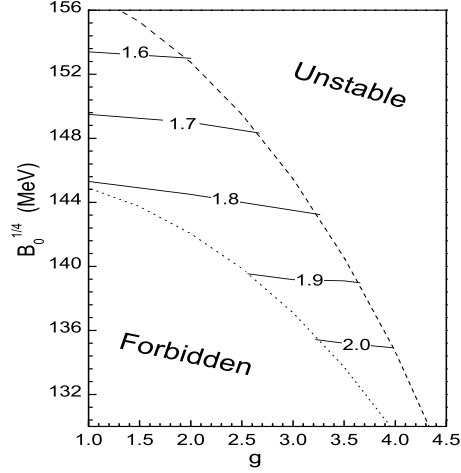


Figure 8: The contour plots of the maximum mass of hybrid stars in the panel $(B_0^{1/4}, g)$. Based on the stability window in Fig. 1, the maximums of hybrid stars are shown on each line in the allowed area.

meta-stable or unstable regions of pure quark matter. Otherwise the hybrid star will collapse to a strange star and no mixed phase could exist.

We show that the maximum mass and radius of hybrid stars are controlled by the equation of state of quark matter [48] rather than that of the nuclear model. Or more exactly in the present framework, they are mainly controlled by the coupling constant g and bag constant B_0 in the quasiparticle model. For a smaller coupling constant, the maximum mass is $1.54 M_\odot$ with radius about 9.64 km. The larger coupling constant will broaden the range of the mixed phase and increase the maximum mass of a hybrid star up to $2.0 M_\odot$. So the quark matter with strong coupling can meet the constraint at high density in compact stars [25] and corroborate the “masquerade effect” in the previous studies [23]. For even high density, the possible CFL matter, especially the magnetized CFL matter [49], should be considered, which will be investigated in our future work.

The authors would like to thank support from the National Natural Science Foundation of China (11005071 and 11135011) and the Shanxi Provincial Natural Science Foundation (2011011001).

References

- [1] J. S. Read, B. D. Lackey, B. J. Owen, and J. L. Friedman, Phys. Rev. D **79** (2009) 124032.
- [2] A. R. Bodmer, Phys. Rev. D **4** (1971) 1601.
- [3] E. Witten, Phys. Rev. D **30** (1984) 272.
- [4] H. C. Liu and G. L. Shaw, Phys. Rev. D **30** (1984) 1137.
- [5] H. J. Crawford, M. S. Desai, and G. L. Shaw, Phys. Rev. D **45** (1992) 857.
- [6] G. Lugones and J. E. Horvath, Phys. Rev. D **66** (2002) 074017.
- [7] M. S. Berger and R. L. Jaffe, Phys. Rev. C **35** (1987) 213.
- [8] J. Madsen, Phys. Rev. D **47** (1993) 5156.
- [9] J. Schaffner-Bielich, C. Greiner, A. Diener, and H. Stoecker, Phys. Rev. C **55** (1997) 3038.
- [10] J. Madsen, Phys. Rev. Lett. **87** (2001) 172003.
- [11] C. Alcock, E. Farhi, A. Olinto, Astrophys. J. **310**(1986) 261.

- [12] P. Haensel, J. L. Zdunik, and R. Schaeffer, *Astron. Astrophys.* **160** (1986) 121.
- [13] X. Y. Lai, R. X. Xu, *Astropart. Phys.* **31** (2009) 128.
- [14] I. Bombaci, P. K. Panda, C. Providencia, and I. Vidaña, *Phys. Rev. D* **77** (2008) 083002.
- [15] N. K. Glendenning, *Compact Stars* (New York: Springer) (1996).
- [16] A. Goyal, *Pramana* **62** (2004) 753-756.
- [17] M. Stejner and J. Madsen, *Phys. Rev. D* **72** (2005) 123005.
- [18] M. Alford and S. Reddy, *Phys. Rev. D* **67** (2001) 074024.
- [19] T. Klahn et. al, *Phys. Lett. B* **654** (2007) 170.
- [20] P. K. Sahu and A. Ohnishi, *Nucl. Phys.* **A691** (2001) 439.
- [21] H. Shen, *Phys. Rev. C* **65** (2002) 035802;
F. Yang, H. Shen, *Phys. Rev. C* **77** (2008) 025804.
- [22] G. F. Burgio, M. Baldo, P. K Sahu, and H. J Schulze, *Phys. Rev. C* **66** (2002) 025802.
- [23] M. Alford, M. Braby, M. Paris, and S. Reddy, *Astrophys. J.* **629** (2005) 969.
- [24] J. E. Trumper, V. Burwitz, F. Haberl, and V. E. Zavlin, *Nucl. Phys. B(Proc. Suppl)* **132** (2004) 560.
- [25] T. Klahn et. al., *Phys. Rev. C* **74** (2006) 035802.
- [26] F. Ozel, *Nature* **441** (2006) 1115.
- [27] R. B Wiringa, V. Fiks, and A. Fabrocini, *Phys. Rev. C* **38** (1988) 1010.
- [28] G. X. Peng, A. Li, and U. Lombardo, *Phys. Rev. C* **77** (2008) 065807.
- [29] P. K. Sahu, *Phys. Rev. C* **62** (2000) 045801.
- [30] N. K. Glendenning, *Z. Phys. A* **327** (1987) 295.
- [31] T. Niksic, D. Vretenar, P. Finelli, and P. Ring, *Phys. Rev. C* **66** (2000) 024306; G. A. Lalazissis, T. Niksic, D. Vretenar, and P. Ring, *Phys. Rev. C* **71** (2005) 024312.
- [32] S. F. Ban, J. Li, S. Q. Zhang, H. Y. Jia, J. P. Sang, and J. Meng, *Phys. Rev. C* **69** (2004) 045805.
- [33] S. Chakrabarty, S. Raha and B. Sinha, *Phys. Lett. B* **229** (1989) 112; O. G. Benvenuto and G. Lugones, *Phys. Rev. D* **51** (1995) 1989; G. X. Peng, H. C. Chiang, J. J. Yang, and B. Liu, *Phys. Rev. C* **61** (1999) 015201; Y. Zhang, R. K. Su, *Phys. Rev. C* **67** (2003) 015202; M. Modarres, H. Gholizade, *Physica A* **387** (2008) 2761.
- [34] K. Schertler, C. Greiner, M. H. Thoma, *Nucl. Phys.* **A616** (1997) 659.
- [35] X. J. Wen, Z. Q. Feng, N. Li, and G. X. Peng, *J. Phys. G* **36** (2009) 025011; X. J. Wen, J. Y. Li, J. Q. Liang, and G. X. Peng, *Phys. Rev. C* **82** (2010) 025809.
- [36] X. J. Wen, S. Z. Su, D. H. Yang, and G. X. Peng, *Phys. Rev. D* **86** (2012) 034006.
- [37] G. Baym, C. Pethick, and P. Sutherland, *Astrophys. J.* **170** (1971) 299.
- [38] S. B. Ruster, M. Hempel, and B. J. Schaffner, *Phys. Rev. C* **73** (2006) 035804.
- [39] R. Manka, I. Bednarek, and G. Przybyla, *Phys. Rev. C* **62** (2000) 015802.
- [40] R. Manka, and I. Bednarek, *J. Phys. G* **27** (2001) 1975.
- [41] I. Bednarek, and R. Manka, *Int. J. Mod. Phys. D* **10** (2001) 607.
- [42] A. R. Bodmer, *Nucl. Phys.* **A526** (1991) 703.
- [43] M. Alford, K. Rajagopal, S. Reddy, and F. Wilczek, *Phys. Rev. D* **64** (2001) 074017.
- [44] B. K. Agrawal, *Phys. Rev. C* **81** (2010) 034323.
- [45] R. D. Pisarski, *Nucl. Phys.* **A498** (1999) 423c; J. P. Blaizot, and J. Y. Ollitrault, *Phys. Rev. D* **48** (1993) 1390.
- [46] C. Maieron, M. Baldo, G. F. Burgio, and H. J. Schulze, *Phys. Rev. D* **70** (2004) 043010.
- [47] P. B. Demorest, T. Pennucci, S. M. Ransom, M. S. E. Roberts, and J. W. T. Hessels, *Nature*, **467**, 1081 (2010); C. H. Lenzi and G. Lugones, *Astrophys. J.* **759** (2012) 57.
- [48] G. Narain, B. J. Schaffner, and I. N. Mishustin, *Phys. Rev. D* **74** (2006) 063003.
- [49] L. Paulucci, E. J. Ferrer, Vivian de la Incera, and J. E. Horvath, *Phys. Rev. D* **83** (2011) 043009.